J. Membrane Biol. 68, 37–46 (1982)

The Journal of
Membrane Biology

Computer Simulation and Interpretation of ^{45}Ca Efflux Profile Patterns

André B. Borle, Takashi Uchikawa, and Julius H. Anderson

Department of Physiology and Department of Pharmacology, University of Pittsburgh School of Medicine, Pittsburgh, Pennsylvania 15261

Summary. Stimulations or inhibitions by various agents of ^{45}Ca efflux from prelabeled cells or tissues display distinct and reproducible profile patterns when the results are plotted against time as fractional efflux ratios (FER). FER is the fractional efflux of ^{45}Ca from stimulated cells divided by the fractional efflux from a control unstimulated group. These profile patterns fall into three categories: peak patterns, exponential patterns, and mixed patterns. Each category can be positive (stimulation) or negative (inhibition). The interpretation of these profiles is difficult because ^{45}Ca efflux depends on three variables: the rate of calcium transport out of the cell, the specific activity of the cell compartment from which the calcium originates, and the concentration of free calcium in this compartment. A computer model based on data obtained by kinetic analyses of ^{45}Ca desaturation curves and consisting of two distinct intracellular pools was designed to follow the concentration of the traced substance (^{40}Ca), the tracer (^{45}Ca), and the specific activity of each compartment before, during, and after the stimulation or the inhibition of calcium fluxes at various pool boundaries. The computer model can reproduce all the FER profiles obtained experimentally and bring information which may be helpful to the interpretation of this type of data. Some predictions of the model were tested experimentally, and the results support the views that a peak pattern may reflect a sustained change in calcium transport across the plasma membrane, that an exponential pattern arises from calcium mobilization from an internal subcellular pool, and that a mixed pattern may be caused by a simultaneous change in calcium fluxes at both compartment boundaries.

Key words Ca efflux · computer simulation · ^{45}Ca profiles

Introduction

Cytosolic free calcium is the transducer of many stimulus-response couplings in a wide variety of cells. Unfortunately, methods to measure ionized calcium in the cytosol of small mammalian cells are not yet readily available. Many investigators have measured the efflux of ^{45}Ca from prelabeled cells as a probe to estimate relative changes in intracellular calcium activity, assuming that the efflux of calcium out of the cells is directly related to the cytosolic concentrations of ionized calcium. Figure 1 shows several examples selected from many such experiments published in the literature [10, 12]. One striking feature of all these experiments is that most if not all the profiles of ^{45}Ca efflux obtained after a given stimulus fall into three distinct patterns: (i) a sudden sharp rise in tracer outflow followed by a slower return to the control levels; this can be called a *peak pattern* (Fig. 1*A*); (ii) a gradual rise in ^{45}Ca efflux that reaches a plateau exponentially and remains at that stimulated level as long as the stimulus is applied; this can be called an *exponential pattern* (Fig. 1*B*); and (iii) a mixture of the two previous patterns which can be called a *mixed pattern* (Fig. 1*C*). Inhibition of ^{45}Ca efflux can be observed as well and these profiles can also be divided into the same three categories: (i) negative peak pattern, (ii) negative exponential pattern (Fig. 1*D*), and (iii) negative mixed pattern. The interpretation of these profile patterns is not easy. Peak patterns are often explained as a transient stimulation of calcium efflux out of the cells; exponential patterns are sometimes assumed to reflect a slow, delayed response to a given stimulus, while mixed patterns are interpreted as temporally biphasic responses. Although these interpretations may be correct, they are not necessarily so because the efflux of ^{45}Ca from cells depends on several independent parameters: the unidirectional transport of ^{40}Ca from the cytosol to the cell environment, the cytosolic free calcium, and the calcium specific activity of the cytosolic pool. For example, the fall in ^{45}Ca efflux which characterizes the peak pattern may be due to a sharp drop in cytosolic calcium specific activity and not to a return of the stimulated ^{40}Ca efflux to control levels. It is, of course, technically impossible to measure each of these variables during a desaturation experiment. However, a computer model representing the calcium pools and the calcium fluxes measured in isolated cells might be able to give some clues about the kinetic properties and behavior of such systems.

0022-2631/82/0068-0037 $02.00

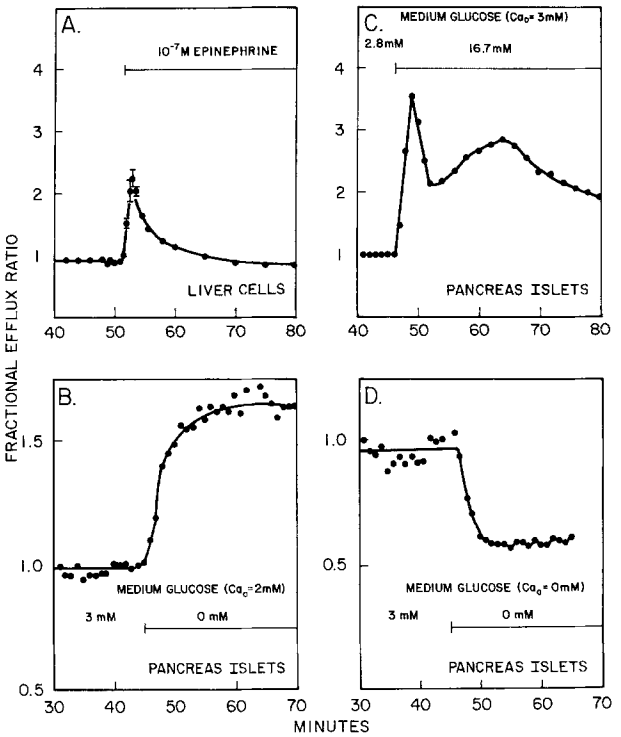

Fig. 1. Selected ^{45}Ca fractional efflux profiles representing the basic patterns. (*A*): *Peak pattern* obtained in isolated liver cells after addition of 10^{-7} M epinephrine (from R.K. Studer and A.B. Borle, *in preparation*). (*B*): *Positive exponential pattern* obtained in pancreatic islets after a decrease in perfusate glucose concentration from 3 to 0 mM in the presence of 2 mM calcium (redrawn as FER from Malaisse et al. [12]). (*C*): *Positive mixed pattern* obtained in pancreatic islets after a rise in perfusate glucose concentration from 2.8 to 16.7 mM in the presence of 3 mM calcium (redrawn as FER from Kikuchi et al. [10]). (*D*): *Negative exponential pattern* obtained in pancreatic islets after a decrease in perfusate glucose concentration from 3 to 0 mM in the absence of extracellular calcium and in the presence of EGTA (redrawn as FER from Malaisse et al. [12])

The objectives of this paper are (i) to describe the method to obtain clear ^{45}Ca efflux profile patterns by calculating fractional efflux ratios; (ii) to describe the computer model representing the calcium compartments of the cells and their calcium exchange, (iii) the computer simulation of tracer desaturation profiles, and (iv) the testing of the model predictions by further experimentation.

Materials and Methods

^{45}Ca Desaturation

Cultured cells, freshly isolated cells, and organ slices can be used to study ^{45}Ca desaturation profiles. In this paper, monkey or bovine kidney cells cultured as monolayer, freshly isolated rat kidney cells, or rat kidney slices were prepared with methods already published [7, 14, 17]. The cells or the slices are preincubated for 1 hr in physiologic buffers (usually Krebs Henseleit bicarbonate buffer with 1.3 mM Ca), labeled with ^{45}Ca for exactly

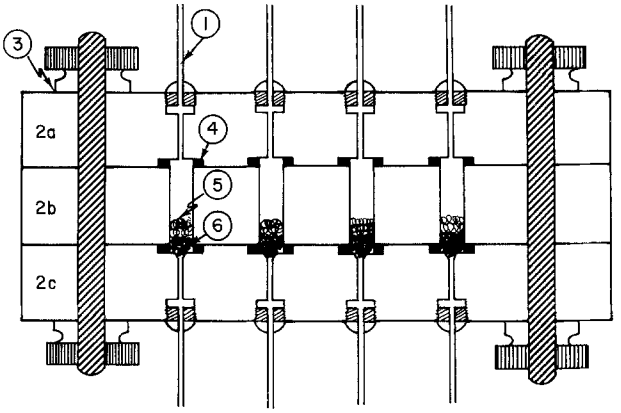

Fig. 2. Lucite perfusion chamber used for ^{45}Ca desaturation from isolated cells or from tissue slices. 1: Specially machined 18 gauge steel hypodermic needles. 2*a*, *b*, *c*: Plastic Lucite block 13.5 × 5.5 × 1.8 cm. 3: Bolt and nuts holding the three pieces of the chamber. 4: 0 ring. 5: Perfusion chamber (5 mm diameter, 18 mm height), capacity 0.35 ml. 6: Layered glasswool plug; bottom layer 2 mm thick tightly packed, upper layer 5 mm thick loosly packed into which cells are placed. The chambers are perfused downwards at a rate of 0.6 ml/min

60 min (1–5 μCi ^{45}Ca/ml) and desaturated in nonradioactive buffer for 2–3 hr. Several methods of desaturation can be used. The cells can be desaturated in a test tube and the medium separated by sequential centrifugation [2] or they can be perfused in flow-through chambers [17]. A new system consisting of four chambers of 0.25 ml capacity (5 mm diameter, 18 mm height) is shown in Fig. 2. After the cells have been labeled in a suspension gently stirred with a magnetic flea, they are transferred to the perfusion chambers as follows: the cell suspension is transferred to a 50-ml centrifuge tube and centrifuged at 200 × *g* for 15 sec. The radioactive medium is decanted, and an aliquot is saved to determine its specific activity. The cell pellet is washed with 40 ml of ice-cold Ca – Mg-free phosphate buffered saline containing glucose [13], resuspended briefly with a wide-mouth pipette, and centrifuged again at 200 × *g* for 15 sec. An aliquot of 60–100 μl of the packed cell pellet (~5 mg cell prot/chamber) is injected with an Eppendorf pipette within a glass wool plug placed in the lower third of the perfusion chamber (*see* Fig. 2). The chamber is closed and perfused with nonradioactive medium at a rate of 0.6 ml/min with a Gilson Minipuls 2. The connections between the medium reservoir, the pump, the perfusion chamber, and the collecting vials are made of Tygon® tubing with an inside diameter of 0.6 to 0.8 mm. The dead space from reservoir to collection vials is 1.5 ml. The effluent is collected in scintillation minivials at intervals varying from 30 sec to 5 min. Each sample in the vials is made up to 3 ml with cold medium to which 4 ml of scintillator is added (New England Nuclear, NEN formula 963). At the end of the experiment the cells of each chamber are collected separately, homogenized with an ultrasonic probe, and aliquots of the homogenates are analyzed for protein, ^{40}Ca and ^{45}Ca [5, 11]. During the desaturation, the medium perfusing two of the chambers is changed to an experimental buffer (change in ionic composition, pH, or addition of hormone, etc.) for a fixed experimental period, while the other chambers are perfused with control medium.

Calculation of the Fractional Efflux Ratio (FER)

The data necessary for the calculations are the radioactivity in each effluent sample CPM(I) (Fig. 3*A*), and the cell radioactivity

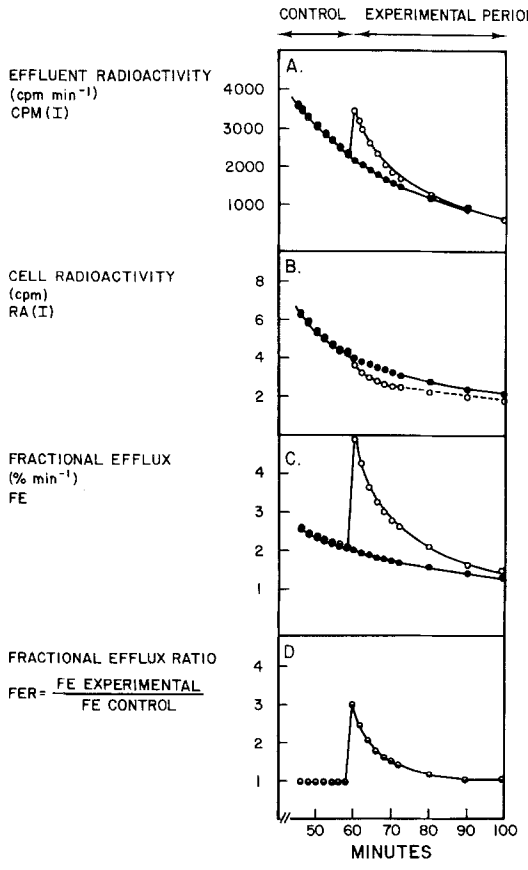

Fig. 3. Conversion of the measured perfusate ^{45}Ca concentration into FER profiles. (*A*): Perfusate ^{45}Ca activity CPM(I) *vs.* time. (*B*): Cell radioactivity RA(I) *vs.* time. (*C*): Fractional ^{45}Ca efflux FE. (*D*): Fractional efflux ratio FER = FE′/FE. ● control group; ○ experimental group

at the end of the experiment CELLCPM. First, the sum of all the radioactivity in each effluent sample plus the radioactivity of the cells at the end of the experiment is taken as the total radioactivity present in the cells at the beginning of the desaturation ΣCPM. The radioactivity of the cells at each time point RA(I) is calculated by sequentially subtracting the effluent radioactivity of each period from ΣCPM or from the cell radioactivity in the previous period RA(I-1):

$$RA(\mathrm{I}) = RA(\mathrm{I\text{-}1}) - \mathrm{CPM(I)}$$

where $RA(0) = \Sigma\mathrm{CPM}$. This is illustrated in Fig. 3*B*.

The fractional efflux (FE) shown in Fig. 3*C* is the radioactivity released per unit time expressed as a percent of the mean cell radioactivity during the collection period $T(\mathrm{I}) - T(\mathrm{I\text{-}1})$:

$$\mathrm{FE(I)} = \{\mathrm{CPM(I)}/[T(\mathrm{I}) - T(\mathrm{I\text{-}1})]\} \times 100/\{[Ra(\mathrm{I}) + RA(\mathrm{I\text{-}1})]/2\}.$$

Finally, the fractional efflux ratio FER is the fractional efflux of the experimental group FE′ divided by the mean fractional efflux of the two control groups FE

$$\mathrm{FER} = \mathrm{FE'/FE}.$$

FER is plotted against time as in Fig. 3*D* and constitutes the profile to be analyzed.

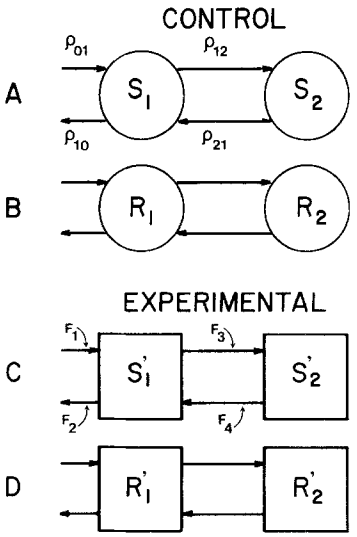

Fig. 4. Computer model designed for the simulation of ^{45}Ca fractional efflux profiles. *See* text for the description of the model

Table 1.

Symbol	Definition
S_i	Amount of traced substance in compartment i
R_i	Amount of tracer in compartment i
X_i	Specific activity of compartment i $X_i = R_i/S_i$
ρ_{ij}	Flux of traced substance from compartments i to j $(i, j = 0, 1, 2; i \neq j)$
k_{ij}	Rate constant of transfer from compartment i to j: $k_{ij} = \rho_{ij}/S_i$ $(i, j = 0, 1, 2; i \neq j)$
′	Primed parameters refer to the stimulated test system
	Unprimed parameters refer to the unstimulated control system

Computer Model of Fractional Efflux Ratio Profiles

Several assumptions have been made in designing the computer model.

Assumption 1. The intracellular exchangeable calcium of perfused isolated cells labeled with ^{45}Ca can be represented by two kinetic pools S_1 and S_2 placed in series with an infinite extracellular compartment S_0 as in the following catenary system:

$$S_0 \underset{\rho_{10}}{\overset{\rho_{01}}{\rightleftharpoons}} S_1 \underset{\rho_{21}}{\overset{\rho_{12}}{\rightleftharpoons}} S_2.$$

Indeed, all cells or tissues (kidney, liver, pancreas, muscle, bone, and pituitary) studied by kinetic analysis of ^{45}Ca desaturation curves have been shown to consist of two intracellular pools of exchangeable calcium [3].

Assumption 2. The extracellular pool of exchangeable calcium (glycocalyx or external membrane binding) detected by the fastest kinetic component of the desaturation curve, can be assumed to be in parallel with the two intracellular pools [16] and can be ignored in the model since its rate constant of exchange (0.44

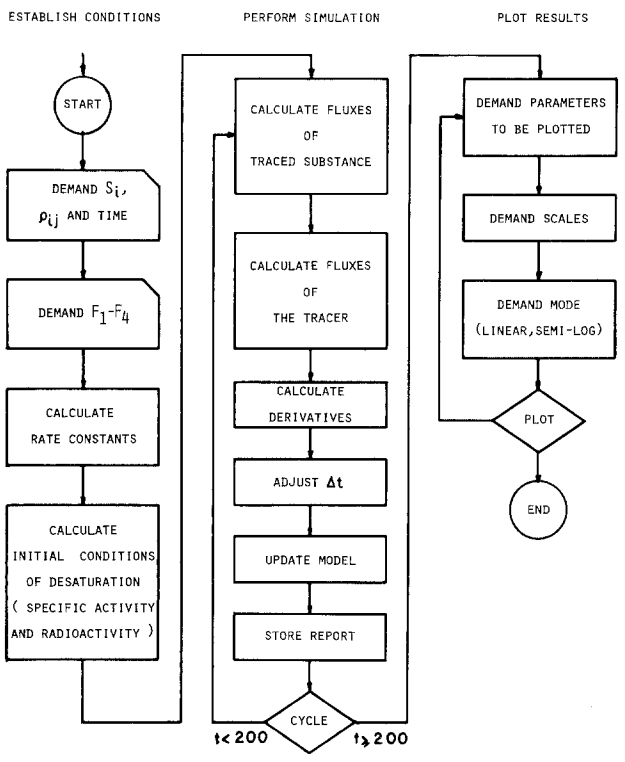

Fig. 5. Flow chart of the computer program designed to simulate fractional efflux profile experiments

min^{-1}) is more than one order of magnitude faster than the two slower kinetic phases. After two time constants (4.5 min), this extracellular compartment can be considered completely desaturated.

Assumption 3. Although calcium fluxes are saturable transport processes, the changes imposed on the model are small (50% decreases or two-fold increases) so that within narrow limits one can assume that k_{ij} is constant and $\rho_{ij}=k_{ij}\cdot S_i$.

Figure 4 shows a representation of the computer model used for the simulations. Table 1 defines all the parameters and symbols used in this analysis.

The model consists of four separate catenary systems: A and B represent the cellular compartments of the traced substance S_1 and S_2 and of its tracer R_1 and R_2 in the control steady-state conditions. C and D represent the equivalent compartments of an experimental cell that undergoes stimulation or inhibition. The specific activity ($X_i=R_i/S_i$) of each compartment i is calculated by the computer. During the simulated labeling period, the specific activity of the extracellular compartment X_0 is arbitrarily set at 1 and kept constant; during the desaturation, X_0 is programmed to be 0 in accord with the conditions prevailing *in vitro* of a constant perfusion with unlabeled medium.

Experimental manipulations are imposed upon the model by altering four factors, F_1 to F_4. F_1 modulates ρ_{01}, F_2 operates on ρ_{10} and F_3 and F_4 regulate ρ_{12} and ρ_{21} respectively. The operation of these modulating factors is very simple: a doubling of ρ_{10} is obtained by setting $F_2=2$, while a 50% reduction in ρ_{12} follows a setting of $F_3=0.5$.

Program

A Fortran IV program was written to simulate the behavior of this model. It consists of approximately 400 Fortran statements and is run on the PROPHET system made available from the NIH Biotechnology Resources Program. To run the program takes approximately 10K of core. Interaction with the computer is accomplished with a Tektronix 4010-1 terminal.

Figure 5 shows the overall flow chart for the computer program. There are three main divisions: (i) establishing initial conditions, (ii) performing the simulation, and (iii) plotting the results.

Initial Conditions

To establish the initial conditions and the parameters of the model, the computer program demands the relevant data (pool sizes and exchange rates). These are furnished from steady-state desaturation data (S_1, S_2, ρ_{01} and ρ_{12}). Before the stimulus is applied, the system is at steady state so that $\rho_{01}=\rho_{10}$ and $\rho_{12}=\rho_{21}$. The rate constants k_{ij} are calculated by the computer program ($k_{ij}=\rho_{ij}/S_i$). The four unidirectional fluxes are increased or decreased by the four different factors F_1 to F_4 which modulate the flux equations. Before the stimulus is applied, the factors have a value of 1. During a stimulation, single or multiple factors can be altered independently. This information is provided to the model at the beginning of the program. Finally, the computer model requests the lengths of time of (i) the labeling period, (ii) the control desaturation period, (iii) the experimental period during which the stimulus is applied, and (iv) the recovery period after cessation of the stimulus. To save computer time, the initial values for the specific activities of the various polls are calculated using standard exponential equations.

Simulation

During the actual simulation, the program proceeds by a point-slope approximation method [9]. Using the pool sizes and rate constants, the fluxes of calcium between each pool are calculated. Subsequently the specific activity of each pool is used to calculate the flow of isotope between each pool. The net flow of calcium and isotope into and out of each pool is divided by the pool size to get the derivative of each pool. The size of the time step to be used is then adjusted so that no pool of calcium or isotope changes by more than 1.0% on a given time step. The model is then updated to reflect both total pool changes and specific activity changes. At the end of each 1.0 min of biological time, the program stores the model values in an array for subsequent display. Finally, as long as t is less than 200 min, the program cycles for another time step. Usually about 3000 cycles are needed to accurately simulate the behavior of the model.

During each run, certain ratios are also calculated to help summarize the results. For instance, the time curve relating the tracer released by the compartments S_1+S_2 (representing the cellular compartments) into S_0 (representing the washout medium) is integrated to give the radioactivity left in S_1+S_2 at each time point (simulation of $RA(I)$). The program also calculates the fractional tracer efflux which is the radioactivity released in S_0 as a function of the radioactivity left in S_1+S_2 (simulation of FE and FE′). Finally the fractional efflux of the stimulated pools is compared to the fractional efflux of the control pools whose steady state is left unperturbed (simulation of FER). The latter ratio gives the efflux profiles and their specific patterns.

Computer Output

The third phase of the program operation is reached only after completion of the simulation. At the end of a run, the data file

Table 2. Interaction between the operator and the program to establish the initial conditions of the simulation

S1 IN CONTROL
4.7
FLUX1 IN CONTROL
0.15
S2 IN CONTROL
3.0
FLUX2 IN CONTROL
0.028
LABELING TIME
60
CONTROL DESATURATION TIME
60
EXPERIMENTAL DESATURATION TIME
80
% CHANGE
0.01
DT MINIMUM
0.001
DT MAXIMUM
0.1
TYPE FACTORS 1, 2 3, 4 IN EACH LINE
1
2
1
1

The underlined figures are the answers entered by the operator. $S1$ and $S2$ are calcium pool sizes expressed as nmol/mg protein. FLUX1 and FLUX2 are calcium fluxes expressed as nmol/(mg protein)(min). The values given are those determined experimentally from steady-state ^{45}Ca desaturations in kidney cells.

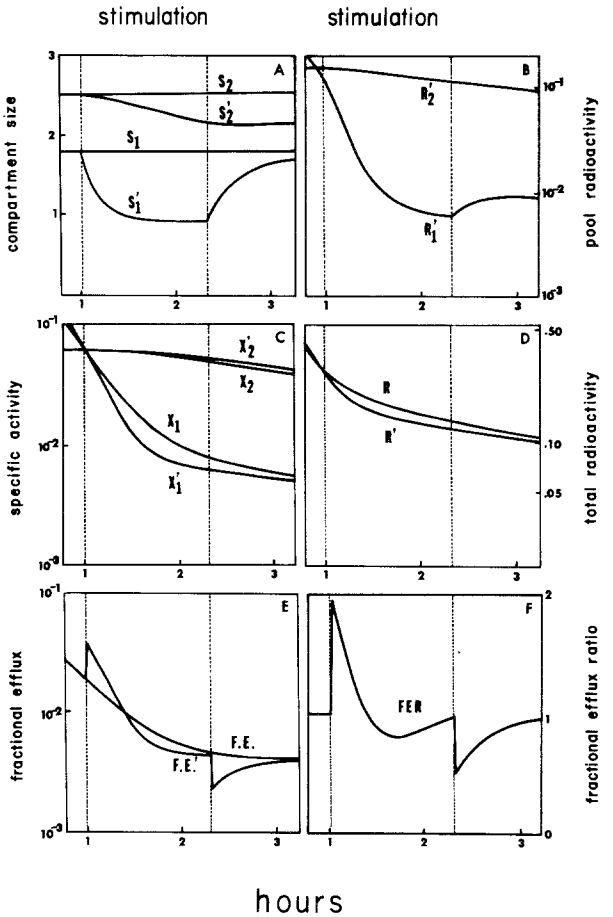

Fig. 6. Some of the parameters computed by the program simulating ^{45}Ca desaturation from isolated cells. The compartment sizes and fluxes assigned to the model are taken from published steady-state experimental values and are given in Table 2. In this simulated experiment, the unidirectional flux ρ_{10} is doubled stepwise at hour 1 and returned to control values 80 min later (F_2 set at 2 from min 60 to 140). (*A*): Compartment size of the control pools S_1 and S_2 and of the stimulated system S'_1 and S'_2. (*B*): Radioactivity of the two pools R'_1 and R'_2 of the stimulated model of the cell. (*C*): Specific activity of the control pools, X_1 and X_2, and of the stimulated system X'_1 and X'_2. (*D*): The total radioactivity of the control pool R ($R=R_1+R_2$) and of the test system R' ($R'=R'_1+R'_2$). (*E*): Fractional efflux of both control and test system, FE and FE'. (*F*): Fractional efflux ratio, FER (FER = FE'/FE); the fractional efflux ratios give the specific profile patterns shown in Fig. 7

has arrays recording the values of 15 different parameters at each of 200 time points. One can select the parameter to plot and specify the scale factors and whether to use linear or semi-log plots. Various combinations of plots can be repeatedly displayed using the results of a single simulation run.

For example, from the data file computed by the program, the following parameters can be displayed or plotted against time: (i) S'_1 and S'_2, the pool size of traced substance before, during, and after the stimulation; (ii) R_1 and R_2, the radioactivity of the control compartments in steady state, unstimulated conditions; (iii) R'_1 and R'_2, the radioactivity of the stimulated system; (iv) X_1, X_2, X'_1 and X'_2, their respective specific activity; (v) the fractional efflux of tracer FE and FE' and their ratios FER. As long as the graph coordinates are compatible, several parameters can be graphed on the same plot. The Fortran program performs Tektronix graphics by making calls to NASUS, a MACRO plot routine supplied for PROPHET by Bolt Beranek and Newman, Inc., Cambridge, Mass.

Sample Run

To illustrate the interaction between the operator and the computer, the following experiment will be simulated: two suspensions of isolated kidney cells are labeled for 60 min with ^{45}Ca. The cells are then desaturated for 180 min. The experimental conditions of the control group are kept constant throughout the desaturation period. In the test group a stimulus which doubles the unidirectional efflux ρ_{10}, (from S_1 to the washout medium) is applied 60 min after the beginning of the desaturation and ρ_{10} is kept elevated for the following 80 min. After the 80-min test period, the stimulus is stopped, ρ_{10} returns to the control levels, and the desaturation is followed for a recovery period of 60 min. To accomplish that, the factor F_2 has to be increased from its control value of 1 to the test value of 2 from min 60 to min 140 of the desaturation. Table 2 shows the interaction between the operator and the program as displayed on the terminal screen. Figure 6 presents the plots of all the parameters computed by the program for control and test conditions: (i) the changes in the

compartment size of each pool; (ii) their radioactivity; (iii) their specific activity; (iv) the total radioactivity of both pools; (v) their fractional efflux; and (vi) the fractional efflux ratio or efflux profile.

Results

Computer simulations of tracer desaturation profiles were obtained by increasing or decreasing single unidirectional fluxes by a factor of 2 for 80 min. Figure 7 shows six basic profile patterns. When the efflux ρ_{10} from the fast peripheral compartment S_1 to the medium S_0 increased twofold at min 60 of the desaturation, a typical peak pattern is observed (Fig. 7*A*). The tracer efflux or FER rises steeply and then returns to baseline despite the fact that the efflux of the traced substance is maintained at its stimulated level throughout the experimental period of 80 min. When the stimulation is stopped and the efflux ρ_{10} is returned to its control level, one observes a negative peak. This fall in FER occurs in spite of the fact that ρ_{10} is identical to the control group.

When the same unidirectional flux ρ_{10} is decreased 50%, a negative peak pattern is observed (Fig. 7*B*). FER drops immediately then the tracer efflux returns toward baseline, although ρ_{10} is kept depressed at the same low level throughout the experimental period. When the inhibition is released and ρ_{10} is returned to normal, a positive peak pattern is obtained. This positive peak pattern occurs when ρ_{10} of the experimental group is identical to the control efflux.

When efflux ρ_{21} from the central slow compartment S_2 to the peripheral fast compartment S_1 is increased by a factor of 2, an exponential rise in FER is obtained (Fig. 7*C*). This slow, progressive rise in tracer efflux occurs even if the flux ρ_{21} is sharply increased, stepwise, at 60 min.

When ρ_{21} is returned stepwise again to its control level, FER returns exponentially to its control level. The opposite occurs with a 50% inhibition of ρ_{21} followed at 80 min by a return to control levels (Fig. 7*D*): an exponential fall of FER which remains depressed throughout the experimental period followed by an exponential rise after the end of the inhibition.

When the two fluxes ρ_{10} and ρ_{21} are stimulated simultaneously, both by a factor of 2, a mixed pattern of FER is observed (Fig. 7*E*), which is the sum of the tracing obtained by stimulating each flux singly. A 50% inhibition of both ρ_{10} and ρ_{21} produces a negative mixed pattern, not unlike a negative square wave (Fig. 7*F*): FER falls abruptly, remains depressed during the inhibition, and rises sharply back to control levels at the end of the experimental period.

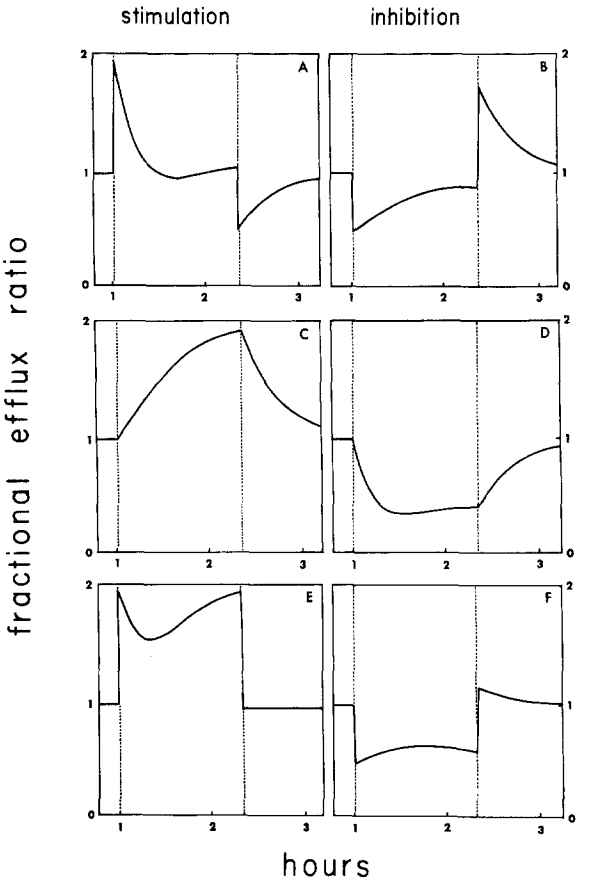

Fig. 7. Computer simulated tracer desaturation profiles. (*A*): Pattern obtained from a twofold stimulation of ρ_{10}, the efflux from the fast peripheral compartment S_1 to the medium S_0 (F_2 set at 2 from min 60 to 140); (*B*): Pattern obtained from a 50% inhibition of ρ_{10} (F_2 set at 0.5); (*C*): Pattern obtained by a twofold stimulation of ρ_{21}, the efflux from the slow compartment S_2 to the fast compartment S_1 (F_4 set at 2); (*D*): Pattern obtained from a 50% inhibition of ρ_{21} (F_4 set at 0.5); (*E*): Pattern obtained from a twofold stimulation of ρ_{10} and of ρ_{21} (F_2 and F_4 set at 2); (*F*): Pattern obtained from a 50% inhibition of ρ_{10} and ρ_{21} (F_2 and F_4 set at 0.5)

Figure 8 presents a summary of single stimulations or inhibitions of each individual flux, simultaneous stimulations of any two fluxes, simultaneous inhibition of any two fluxes and all possible combinations of the stimulation of any one flux plus the inhibition of another.

Interpretation of ^{45}Ca Fractional Efflux Profiles

In this computer model, the reproducibility of the basic patterns of ^{45}Ca fractional efflux is remarkably immune from changes in the assigned pool sizes of S_1 or S_2, in the absolute rates of exchange ρ_{ij}, in the time of labeling (i.e., relative specific activity of S_1 and S_2), and in the time of the stimulation or inhibition (early desaturation or late desaturation).

Several conclusions can be drawn from these

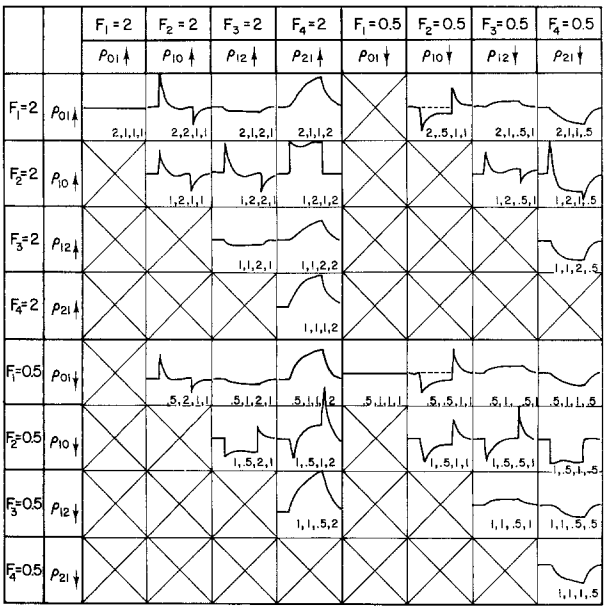

Fig. 8. Summary of FER profile predicted by the computer model. All stimulations are twofold ($F_i=2$, $i=1-4$), and all inhibitions are 50% reductions ($F_i=0.5$, $i=1-4$). Left upper panel: single and double stimulations. Right upper and left lower panels: mixed stimulations and inhibitions. Right lower panel: single and double inhibitions. The pools sizes, fluxes, and time sequence used are those given in Table 2. The four numbers at the lower right corner of each box indicate the values of F_1, F_2, F_3, and F_4, respectively, during the experimental period

computer simulations of ^{45}Ca efflux profiles. First, it is apparent that the positive peak patterns frequently observed after the introduction of a given stimulus do not necessarily reflect a transient increase in calcium efflux. Such a pattern can also represent a stimulation sustained throughout the experimental period. The fall in the fractional efflux of tracer may be due to the faster drop in specific activity of the rapidly exchanging intracellular compartment of the stimulated cell compared to the control. This is clearly shown in Fig. 6*C* where X_1' drops much faster than X_1. This is also true for the negative peak patterns which do not necessarily represent transient inhibitions but may reflect sustained inhibitions with different rates of decay of intracellular specific activity.

Secondly, a progressive or slow rise in ^{45}Ca fractional efflux may not reflect a slow or delayed stimulation reaching a maximum only after same elapsed time. It can represent an immediate and maximal stimulation of Ca efflux from an internal compartment. Thus a rise in ^{45}Ca efflux may appear later than the maximal stimulation of a calcium-triggered function if the source of calcium is an intracellular compartment. It would be wrong to conclude that the two phenomena are unrelated.

Thirdly, a mixed pattern of ^{45}Ca fractional efflux (e.g., Figs. 1*C* and 7*E*) does not necessarily mean that the stimulus has a biphasic effect: a fast effect followed by a delayed action. It may also reflect a simultaneous effect on two different fluxes at the boundaries of different calcium compartments.

One surprising prediction of the computer model is that a stimulation or an inhibition of calcium influx into the fast compartment (a rise or a fall in ρ_{01}) does not produce any changes in fractional efflux (*see* Fig. 8). Moreover, a change in ρ_{01} superimposed on any other stimulation or inhibition of the three other fluxes does not alter the characteristic pattern of FER (Fig. 8).

Test of the Computer Model

Kinetic analyses of steady-state ^{45}Ca desaturation curves from isolated cells or tissue slices have consistently shown three kinetic components: two intracellular pools of exchangeable calcium and one extracellular compartment. The fast intracellular pool has been identified with the cytosolic compartment, while the slowest compartment has been associated with subcellular organelles, mainly the mitochondria [3, 7, 14, 16, 17]. The steady-state calcium exchange between the mitochondrial pool and the cytosol or the fluxes between the cytosol and the extracellular compartment across the plasma membrane have been shown to be altered singly or together by a variety of experimental conditions. To test the prediction of the computer model, fractional efflux profiles were obtained with stimuli or experimental conditions known to alter these fluxes.

1. Calcium efflux across the plasma membrane. The model predicts that an inhibition of calcium efflux across its outer boundary (ρ_{10}) should produce a negative FER peak pattern, while a stimulation of ρ_{10} should give a positive FER peak pattern. In our model, this outer boundary represents the cell plasma membrane. A series of recent experiments has shown that, in renal cells, lowering the extracellular Na or replacing it entirely with choline or tetraethylammonium ions decreases the steady-state efflux of calcium across the plasma membrane without affecting the mitochondrial calcium, the slowly exchangeable calcium pool associated with mitochondria, or the steady-state calcium exchange between the mitochondria and the cytosolic pool [4]. One would predict that such conditions would produce typical FER peak patterns. Figure 9 shows the effect of reducing extracellular Na to zero and substituting choline in a Hepes buffered Krebs Henseleit medium perfusing prelabeled rat kidney slices. When extracellular Na is totally replaced by choline, there is an immediate 15% drop in FER; when Na is reintroduced in the medium, the fractional efflux rises then falls. Both inhibition and stimulation have the

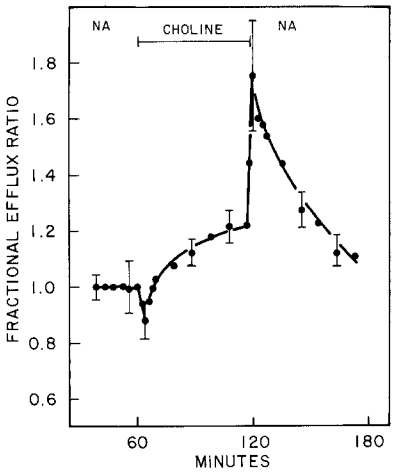

Fig. 9. FER profile obtained by totally replacing extracellular Na by choline from min 60 to 120, in the medium perfusing rat kidney slices. The slices were perfused in flow-through chambers with Krebs Henseleit Hepes buffers with 1.3 mM Ca [4]. Mean ± SE of 6 experiments

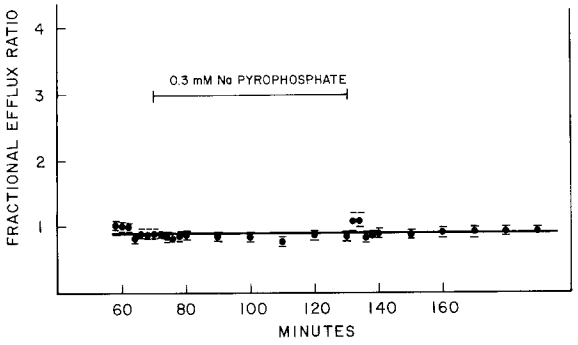

Fig. 10. FER profile obtained by the addition of 0.3 mM pyrophosphate from min 70 to 130 in the medium perfusing rat kidney slices. The slices were perfused in flow-through chambers with Krebs Henseleit Hepes buffers with 1.3 mM Ca. Mean ±SE of 9 experiments

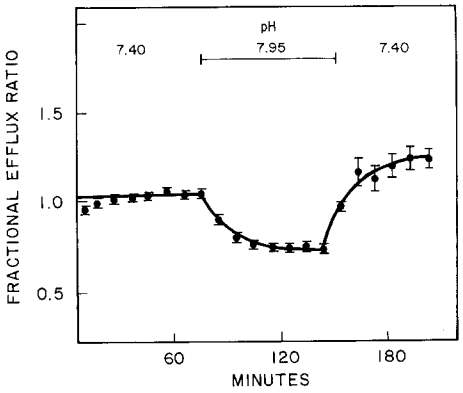

Fig. 11. FER profile obtained by decreasing the pCO_2 from 5 to 1.25% from min 70 to 140 in the Krebs Henseleit bicarbonate buffer (Ca = 1.3 mM) bathing cultured bovine kidney cells. The pH rose from 7.4 to 7.95 during the experimental period. The cells were incubated as a suspension in polycarbonate tubes and desaturated by sequential centrifugation [2]. Mean ±SE of 4 experiments

typical peak patterns expected from the changes in calcium efflux across the plasma membrane obtained in the steady-state experiments.

2. Calcium influx across the plasma membrane. The model predicts that a stimulation or an inhibition of ρ_{01} does not alter the fractional efflux of ^{45}Ca so that no FER pattern is obtained. We have shown in the past that low concentrations of pyrophosphate, 0.1 to 0.5 mM, produce a massive net shift of calcium into kidney cells [2] and increase all intracellular calcium compartments [1]. In spite of this stimulation of calcium influx, one would predict from our model that no change in FER should be observed. Figure 10 shows that, indeed, 0.3 mM pyrophosphate, which significantly increases calcium influx [2], does not produce any FER pattern.

3. Stimulation of calcium uptake by mitochondria. According to the model, a stimulation of influx ρ_{12} into the inner compartment should produce an exponential fall in FER that should be maintained until the end of the stimulation, which should produce an exponential rise back to control levels. Studer and Borle have shown that increasing the medium pH bathing isolated kidney cells increases intracellular pH and stimulates calcium influx into the mitochondrial pool without affecting calcium transport across the plasma membrane [14]. In addition, a high pH of 7.7 stimulates calcium uptake by isolated rat kidney mitochondria [15]. Figure 11 shows that increasing the pH of a Krebs Henseleit bicarbonate buffer by lowering the pCO_2 from 5 to 1.25%, produces an exponential fall in FER, which returns exponentially to control levels when the pH is restored to 7.4. The rise in intracellular pH produced by a 1.25% CO_2 has been measured to be 7.9 [14].

4. Inhibition of calcium uptake by mitochondria. An inhibition of the influx of calcium into the inner compartment ρ_{12} would produce a positive exponential pattern, according to the computer model. Such an inhibition of calcium influx into mitochondria has been described in kidney cells and in isolated kidney mitochondria when intracellular pH is lowered by decreasing medium pH [14, 15]. Thus an intracellular acidosis should give an exponential rise in FER. Figure 12 shows the effect of increasing the pCO_2 of the gas phase of a Krebs Henseleit bicarbonate buffer bathing isolated kidney cells from 5 to 20%, which has been shown to decrease intracellular pH to 7.11. When the medium pH is lowered to 6.8 the fractional efflux rises exponentially, stays elevated, and when the medium pH is returned to normal, the FER returns to basal levels. This example is not as clear cut as the previous one, because

intracellular acidosis also depresses the steady-state exchange of calcium across the plasma membrane [14]. However, if one assumes that this decreased plasma membrane exchange is a consequence of a decreased influx into the cells, the FER pattern would still be a simple exponential rise since changes in calcium influx do not produce any change in fractional efflux patterns (*see* Fig. 8).

5. *Stimulation of efflux from both cellular compartments.* In our model, the simultaneous stimulation of the two fluxes ρ_{21} and ρ_{10} produces a mixed FER pattern. We have previously shown that cyclic AMP stimulates ^{45}Ca efflux from renal cells [2]. Kinetic analyses of steady-state desaturation curves also indicate that two compartment boundaries are significantly affected: calcium exchange between the mitochondrial pool and the cytosol and calcium transport across the plasma membrane between the cytosol and the cell environment [8]. One would thus predict that cyclic AMP would produce a mixed FER pattern. Figure 13 indeed shows that in rat kidney slices, the addition of 10^{-3} M cyclic AMP stimulates ^{45}Ca efflux: there is an immediate rise which rapidly declines (peak) then a sustained elevation which rapidly subsides when cyclic AMP perfusion is stopped. In these experiments, the slices were perfused with a buffer devoid of calcium so that one must conclude that the ^{45}Ca appearing in the medium must have been mobilized from an intracellular compartment. However, it is impossible to decide whether cyclic AMP stimulates the two fluxes simultaneously or whether calcium efflux out of the cell is a consequence of a rise in cytosolic free calcium induced by its release from an internal compartment.

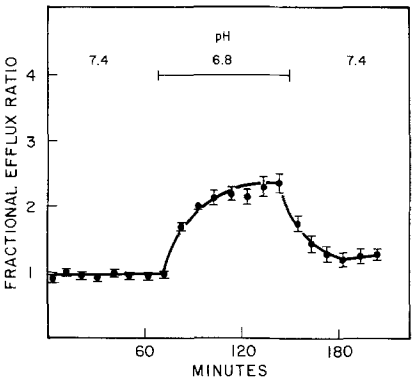

Fig. 12. FER profile obtained by increasing the pCO_2 from 5 to 20% from min 70 to 140 in the Krebs Henseleit bicarbonate buffer bathing cultured bovine kidney cells. The pH fell from 7.4 to 6.8 during the experimental period. The cells were incubated as a suspension in polycarbonate tubes and desaturated by sequential centrifugation [2]. Mean ±SE of 4 experiments

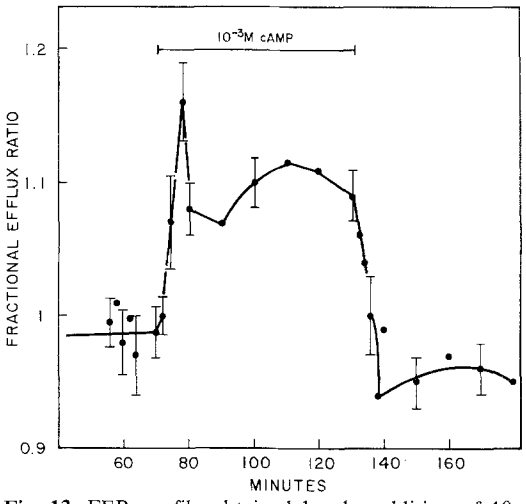

Fig. 13. FER profile obtained by the addition of 10^{-3} M cyclic AMP from min 70 to 130 in the medium perfusing rat kidney slices. The slices were perfused in flow-through chambers with Krebs Henseleit bicarbonate buffers (Ca = 0 mM). Mean ±SE of 7 experiments

Discussion

The measurement of ^{45}Ca fractional efflux is a useful and easy method to study the effects of hormones and other stimuli that affect cellular calcium metabolism.

First, FER profiles can demonstrate whether a stimulus enhances or inhibits calcium efflux from a cell. When properly performed in calcium-free media, such experiments can rule out changes in calcium influx as the first step in the sequence of events which leads to the change in calcium metabolism. For instance, an increase in ^{45}Ca efflux in calcium-free media can only indicate that the source of calcium is intracellular; consequently, the stimulus or its second messenger signal must have an intracellular target site. However, the method by itself cannot precisely define the sequence of events from stimulus to response. Furthermore, an absence of calcium signal (no positive or negative FER profile) does not prove that a stimulus has no action on cellular calcium metabolism: the absence of profile after pyrophosphate administration and the model prediction that changes in calcium influx do not produce any FER pattern are good illustrations. The method can only give qualitative information. Since the specific activity of the cellular compartments cannot be measured during the experiment, the efflux of ^{45}Ca cannot be converted into actual fluxes and no reliable quantitative information can be obtained.

The computer model described in this paper provides some insight about the behavior of the system. Although it is clear that the model is an oversimplification of cellular calcium, it can provide useful information: first a FER peak pattern may in-

dicate that in a two-compartment series system, the stimulus acts primarily at the most peripheral boundary (e.g., plasma membrane). It also shows that the return to control levels of the fractional efflux can be explained by a change in the fast compartment specific activity while the rate of efflux remains stimulated or inhibited. The usual explanation that the effect is transient is another possible explanation.

Second, the model shows that an exponential FER pattern may indicate an immediate change in calcium fluxes across the more central boundary (e.g., mitochondrial membrane) and not necessarily a progressive or delayed action. A mixed pattern may indicate a simultaneous or sequential activation of both boundaries.

In all cases, however, it is impossible to know whether the increased calcium efflux is due to a rise in free calcium in one particular pool S_i or whether it is caused by an increased rate constant k_{ij} which could reflect an increased velocity of a transport process, by a greater passive permeability when the flux is going down its thermodynamic gradient, or by the increased affinity of a possible carrier molecule to calcium. Only the resulting increase in calcium flux can be detected.

The reasonably good fit between the model's predictions and the experimental data is encouraging. Simple peak or exponential patterns may very well indicate the site of action of a stimulus, and the method may provide a nondestructive way of studying events occurring at the boundary of intracellular organelles. However, the identification of this most central compartment can still be the subject of controversy, and it may be different in various cells. It appears that in kidney cells this intracellular central compartment represents mostly mitochondrial calcium [3, 4, 6–8, 14, 17].

There is no reason to believe that the predictions based on results obtained at steady state will always agree with the data derived from FER profiles. Indeed, a stimulus may cause a shift in cell calcium metabolism from one steady state to another. The calcium fluxes and the free calcium of each compartment may be different during the early transient phase and during the stimulated steady state. Since FER profiles reflect this transient phase, some discrepancy can be expected.

In conclusion, fractional efflux profiles can be a useful tool for the study of cell calcium metabolism. A computer model simulating these experiments predicts that effects at specific cell boundaries can be discriminated. Nevertheless, these FER profiles should be only one in an array of methods used to study cellular calcium metabolism.

This work was supported by U.S. Public Health Service grant AM07867 from the National Institute of Health. The PROPHET computer system used for the model and the simulations was made available by the Division of Research Resources of the National Institutes of Health. The technical assistance of Mrs. Mary Wusylko and Sandra Gregor is gratefully acknowledged.

References

1. Borle, A.B. 1971. Calcium transport in kidney cells and its regulation in cellular mechanisms for calcium transfer and homeostasis. G. Nichols, Jr., and R.H. Wasserman, editors. pp. 151–174. Academic Press, New York
2. Borle, A.B. 1975. Methods for assessing hormone effects on calcium fluxes *in vitro*. *In:* Methods in Enzymology, Vol. 39. Hormone Action, part D, Isolated Cells, Tissues and Organ Systems. J.G. Hardman and B.W. O'Malley, editors. p. 513–573. Academic Press, New York
3. Borle, A.B. 1981. Control, regulation and modulation of cell calcium. *Rev. Physiol. Biochem. Pharmacol.* **90**:13–153
4. Borle, A.B. 1982. Effect of sodium on cellular calcium transport in rat kidney. *J. Membrane Biol.* **66**:183–191
5. Borle, A.B., Briggs, F.N. 1968. Microdetermination of calcium in biological material by automatic fluorometric titration. *Anal. Chem.* **40**:339–344
6. Borle, A.B., Clark, J. 1981. Effects of phosphate induced hyperparathyroidism and parathyroidectomy on rat kidney calcium *in vivo*. *Am. J. Physiol.* **241**:*E*136–*E*141
7. Borle, A.B., Uchikawa, T. 1978. Effects of parathyroid hormone on the distribution and transport of calcium in cultured kidney cells. *Endocrinology* **102**:1725–1732
8. Borle, A.B., Uchikawa, T. 1979. Effects of adenosine 3′,5′-monophosphate, dibutyryl adenosine 3′,5′-monophosphate, aminophylline and imidazole on renal cellular calcium metabolism. *Endocrinology* **104**:122–129
9. Garfinkel, D., Ching, S.W., Adelman, M., Clark, P. 1966. Techniques and problems in the construction of computer models of biochemical systems including real enzymes. *Ann. N.Y. Acad. Sci.* **128**:1054–1068
10. Kikuchi, M., Wollheim, C.B., Cuendet, G.S., Renold, A.E., Sharp, G.W.G. 1978. Studies on the dual effect of glucose on ^{45}Ca efflux from isolated rat islets. *Endocrinology* **102**:1339–1349
11. Lowry, O.H., Rosebrough, N., Farr, A., Randall, R. 1951. Protein measurement with the Folin phenol reagent. *J. Biol. Chem.* **193**:265–275
12. Malaisse, W.J., Brisson, G.R., Baird, L.E. 1973. Stimulus-secretion coupling of glucose-induced insulin release: X. Effect of glucose on ^{45}Ca efflux from perfused islets. *Am. J. Physiol.* **224**:389–394
13. Merchant, D.J., Kahn, R.H., Murphy, W.H. 1964. Handbook of Cell and Organ Culture. Burgess, Minneapolis
14. Studer, R.K., Borle, A.B. 1979. Effect of pH on the calcium metabolism of isolated rat kidney cells. *J. Membrane Biol.* **48**:325–341
15. Studer, R.K., Borle, A.B. 1980. The effects of hydrogen ions on the kinetics of calcium transport by rat kidney mitochondria. *Arch. Biochem. Biophys.* **203**:707–718
16. Uchikawa, T., Borle, A.B. 1978. Kinetic analysis of calcium desaturation curves from isolated kidney cells. *Am. J. Physiol.* **234**:R29–R33
17. Uchikawa, T., Borle, A.B. 1978. Studies of calcium-45 desaturation from kidney slices in flow-through chambers. *Am. J. Physiol.* **234**:R34–R38

Received 31 August 1981; revised 4 December 1981